Materials Physics and Mechanics 38 (2018) 26-32 Received: March 16, 2018

EFFECT OF ALUMINA ADDITION ON WELD DEPOSITS MICROSTRUCTURE AT THE WELDING OF CARBON STEEL

E.V. Bobrynina[1*], T.V. Larionova[1], T.S. Koltsova[1], S.A. Ginzburg[2], V.G. Michailov[2]

[1]Peter the Great St.Petersburg Polytechnic University, Russia

[2]Brandenburgische Technische Universität Cottbus-Senftenberg, Germany

*e-mail: bobrynina@inbox.ru

Abstract. The formation of acicular ferrite in the structure of weld deposits when welding carbon steels is often associated with the introduction of nonmetallic additives into the electrode material. Fe–alumina composite powders with alumina particles less than 1 μm were used as a filler for cored welding wire and the influence of aluminum oxide additives up to 2,5 wt.% on the structure of the welded seam was studied. It was shown that the addition of aluminum oxide to the welding wire led to the initiation of the formation of intragranular acicular ferrite in the weld deposit and to a more even distribution of hardness through the zones of weld seam.

Keywords: acicular ferrite; alumina; welding; carbon steel.

1. Introduction

The addition of dispersed oxide particles into ferritic steels significantly improves their mechanical properties at elevated temperatures [1], since the stable at high exploitation temperatures submicron oxide particles inhibit the movement of dislocations and grain growth [1-3]. To date, dispersed-strengthened (DS) steels have been widely discussed in scientific literature as the materials for reactors and gas turbines operating at up to 700°C [1, 4].

On the other hand, the presence of oxide particles in the weld pool often has a beneficial effect on the structure of the weld and on the final properties of the welded products [5-10]. For example, it was shown in [5-7] that the introduction of titanium oxide nanoparticles into electrode coating allowed to modify the structure and to improve the properties of the welded joint. Introduction of 1.2 wt.% of zirconia made it possible to increase the strength of low-carbon steel joints by about 37% [8].

Often, the increase in strength and impact strength at negative temperatures is associated with the presence of acicular ferrite (AF) in the weld structure [8-9]. It is believed that the formation of AF is associated with the presence of nonmetallic inclusions [11-12]. According to literature data [7-12] the formation of AF may be initiated by oxides such as titania, zirconia and others, for example, authors [9], by introducing small additions of titanium oxide, obtained welds with the structure of acicular ferrite.

The possible reasons of the formation of acicular ferrite in the presence of nonmetallic inclusions had been discussed in detail in the works of H. Badeshia, S.S. Babu and R. Honeycombe, and generalized in [11]. The authors show the possible mechanisms for the initiation of acicular ferrite in the presence of oxide particles and conclude that there are many possibilities (nucleation at crystal lattice matching, stimulation of ferrite growth by thermal deformations upon cooling, or the presence of chemical inhomogeneities near the

http://dx.doi.org/10.18720/MPM.3812018_4

inclusion / matrix interface) that help make the nonmetallic phase a heterogeneous site for the nucleation of ferrite. In fact, nonmetallic inclusions tend to consist of many crystalline and amorphous phases, so that it becomes difficult to identify the specific component and mechanism responsible for the initiation of acicular ferrite in each case. It was suggested in [13] that under certain conditions all oxide inclusions should initiate the formation of AF.

In general, despite of the fact that various types of nonmetallic inclusions have already been investigated, inconsistent information prevails about aluminum oxide [14]. Aluminum oxide has been used successfully for the dispersive hardening of materials based on copper, nickel and iron, while it is not actively used as a modifier of the structure of welded joints, despite the good correspondence of the crystal lattices of ferrite and gamma alumina [11]. Therefore, the purpose of this work was to carry out additional studies on the effect of alumina particles on the structure and properties of the welded seam. To produce a powder material with a highly distorted crystal lattice, the most common method was used - grinding in a high-energy mill, which is widely used to create composite powder materials [15].

2. Experimental

Iron and alumina (corundum) powders with a particle size of less than 100 μm have been used as starting materials. The grinding of alumina powder was carried out in 80 ml beakers in a Pulverisette 7 planetary mill. As can be seen from Fig. 1, the initial alumina powder has the average particle size of more than 20 μm. Powder was grinded in the planetary mill at a rotation speed of 400 rpm for 4 h with ceramic balls of 10 mm in diameter, the mass of the sample was 8 g, and balls-to-powder mass ratio was 1:10.

Additional grinding of a mixture of Fe and Al_2O_3, was carried out by milling with balls of hardened steel with a diameter of 10 mm. In order to prevent oxidation, the milling was carried out in an Ar atmosphere. The preparation of the composite powder was carried out in two stages: first was the mixing at 200 rpm for 2 hours, then grinding at 600 rpm also for 2 hours. Alumina content in final powders was varied from 2.5 to 10 wt%.

To create filled welding wires, a steel tube made of Steel 10 was used, the diameter of the tube was 6 mm, the wall thickness was 1 mm, and the initial length was 10-12 cm. A powder was pressed into the steel tube. The wire was rolled by a rolling mill from a starting diameter to 2 mm. After that, the finished flux cored wires were surfacing melted onto the substrate (steel 45) by the argon-arc welding method (I = 200 A).

The study of powder composite materials was carried out on a scanning electron microscope MIRA 3 TESCAN, X-ray diffraction (XRD) analysis was carried out on a DRON-2 diffractometer in monochromatized CuKα radiation. The microstructure of the welded seam (WS) and the heat-affected zone (HAZ) was studied using the metallographic method at x100-x500 magnifications using the Leica-DMI5000 optical microscope and using a Phenom ProX scanning electron microscope. The microhardness was measured on a ZWICK ZHU equipment at a load of 100 H.

3. Results and discussions

The micrographs of the initial and pre-grounded alumina are shown in Fig. 1 (a and b respectively). The powder consists mainly of agglomerated particles with the size of about 2 microns; the size of the individual particles in agglomerates is less than 100 nm. After grinding, alumina is X-ray amorphous (insertion in Fig. 1(b)).

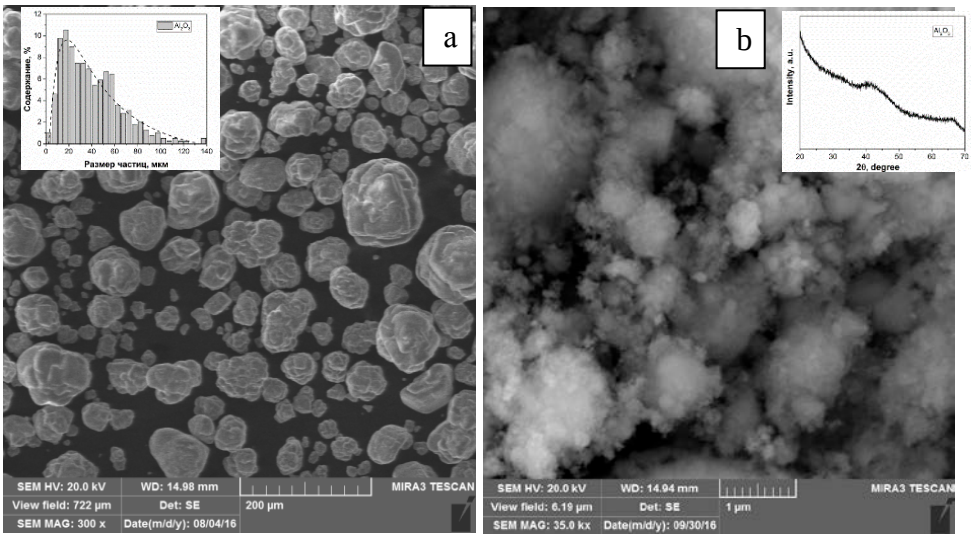

Fig. 1. Micrographs of initial alumina powder (a) and alumina powder after ball milling at 400 rpm for 4h (b). The insertion in Fig (a) shows particle size distribution in the initial powder and in (b) the result of XRD analysis powder after ball milling.

The microphotography and diffractograms of the composite powder Fe-Al_2O_3 are presented in Fig. 2. The results of X-ray diffraction analysis show the presence of reflexes from pure iron, peaks belonging to alumina are not observed. As can be seen in Fig. 2, the increase in the content of aluminum oxide did not affect the position and shape of the iron peaks.

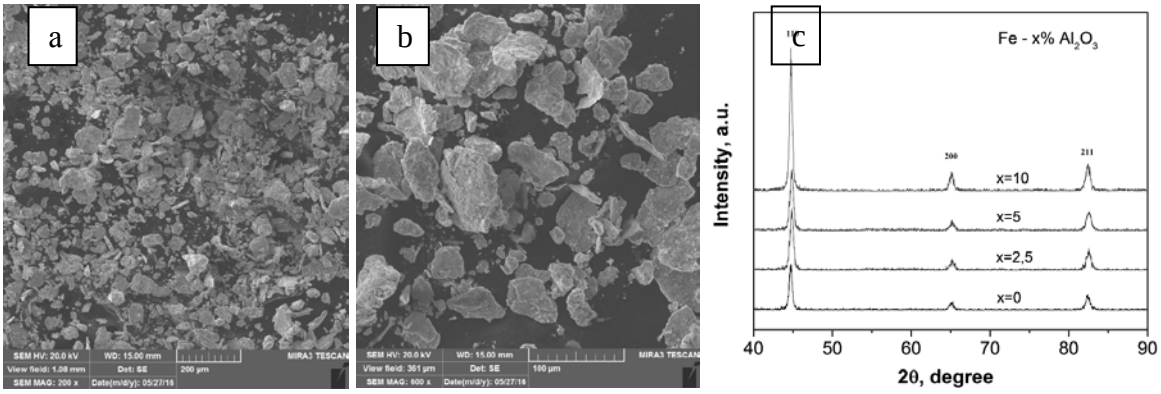

Fig. 2. Micrographs at different magnifications (a, b) и and XDR patterns (c) of composite Fe-Al_2O_3 powders after milling at 600 rpm for 2 h.

According to the procedure described above, the wires with different alumina contents were manufactured from the resulting powder. The final content of alumina in wire was 2.5 mass%, 1.2 wt.% and 0,6 wt% (made from starting powder Fe-10; 5; 2.5 wt% Al_2O_3 respectively). For comparison, the wire with a pure iron powder is prepared.

Surfacing was obtained by the method of argon-arc welding. Figure 3 shows the microstructures of the central zone of the weld.

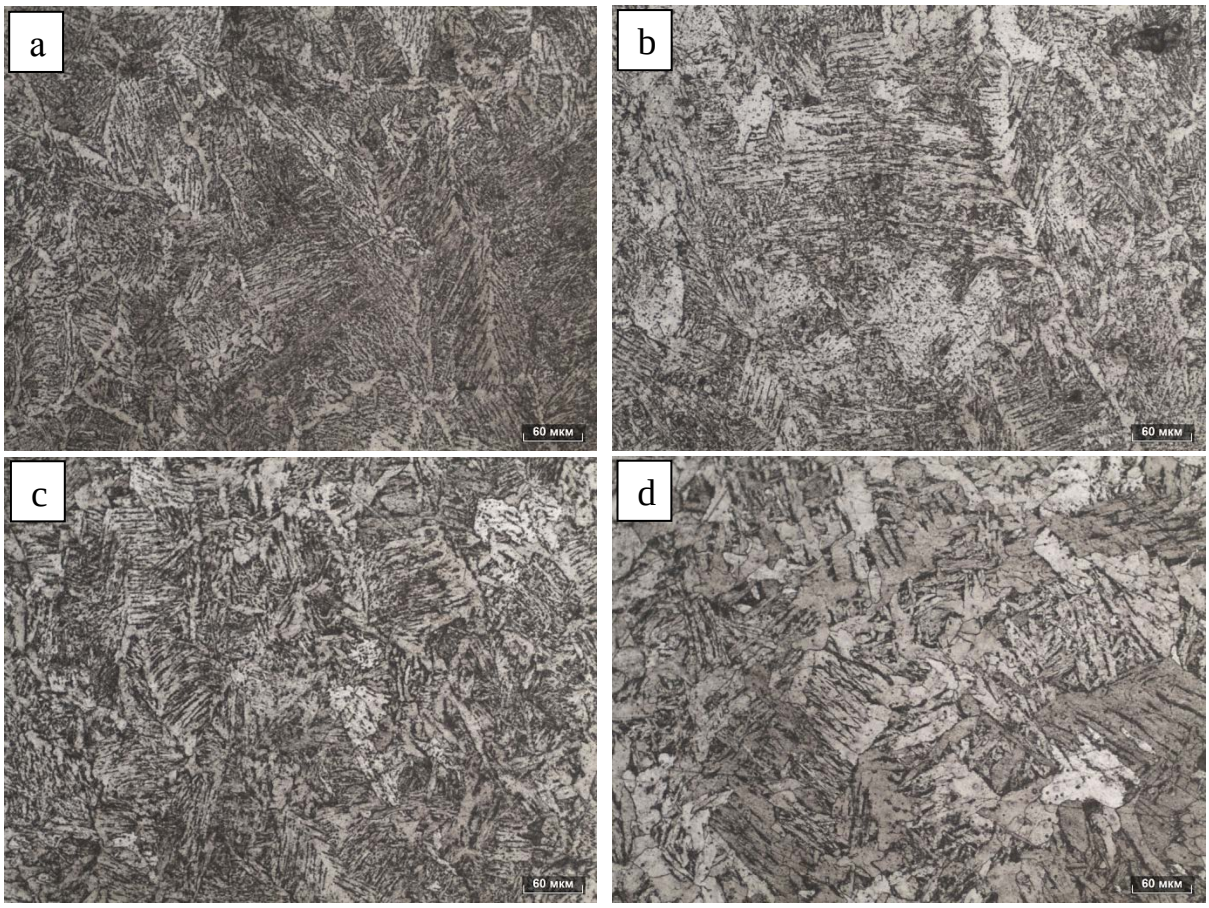

Fig. 3. Microstructure of the central zone of the welded seam. The welds were made by using a welded wire with an aluminum oxide content of 0 (a), 0.6 (b); 1.2 (c) and 2.5 wt% (d).

In structures ferrite along the boundaries of austenite grains, polyhedral ferrite, a bainitic-martensitic structure, and a small amount of acicular ferrite were identified. In the initial seam, when using the wire without the addition of alumina, the main structural constituents are grain-boundary ferrite and a bainitic-martensitic structure. When aluminum oxide is added, polyhedral ferrite appears and its proportion increases with increasing oxide concentration, the proportion of acicular ferrite also increases, with the bainite component practically disappears. An obvious coarsening of the microstructure is also observed.

Figure 4 shows the microstructure of the columnar zone of welded seams. With the addition of aluminum oxide, the columnar structure becomes more pronounced; the size of the structural components significantly increases. The increase of polyhedral ferrite fraction and the decrease in the proportion of the bainitic-martensitic component, together with the general coarsening of the microstructure, can be explained only by a decrease of the cooling rate of the weld pool, which takes place most likely due to a change in the thermophysical characteristics of the electrode and the weld pool when nonmetallic particles are added.

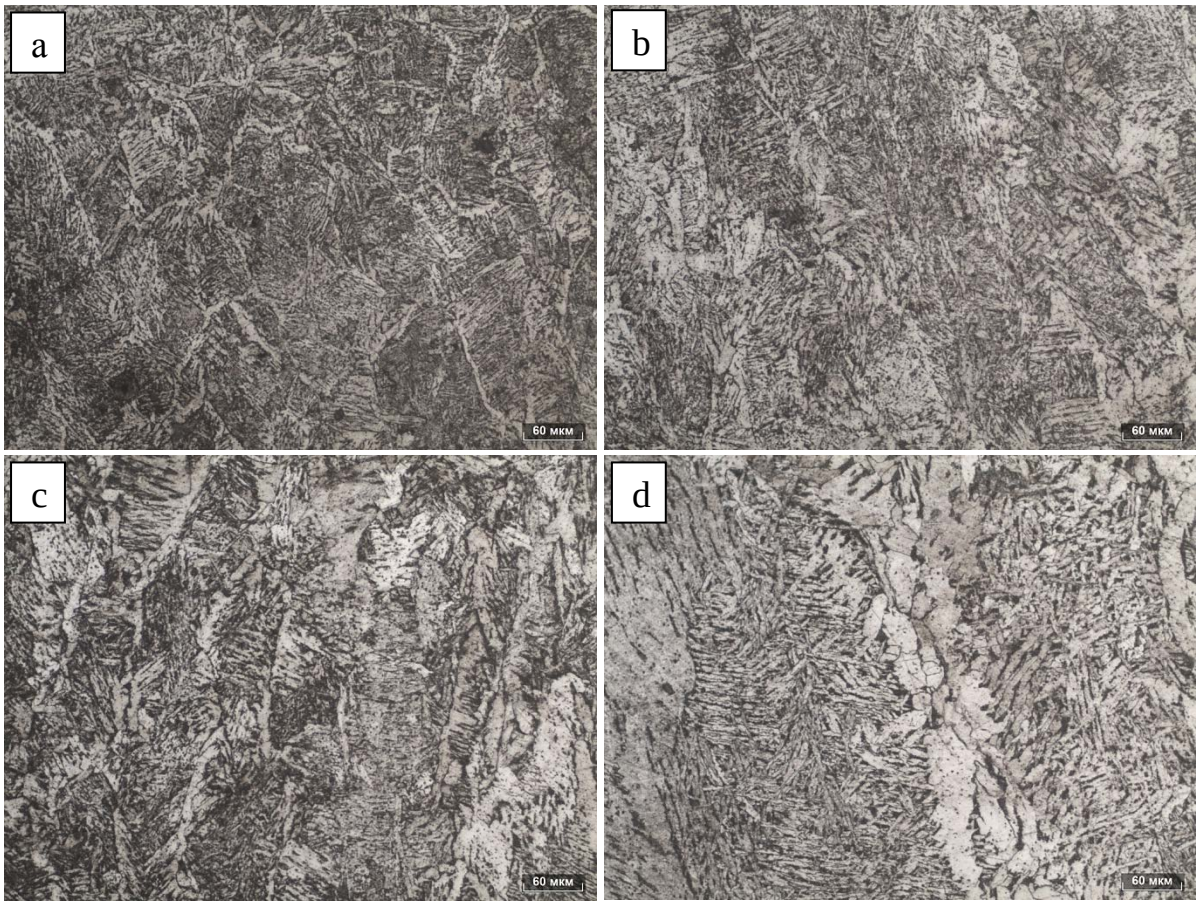

Fig. 4. The microstructure of the weld zone near HAZ made with the use of welded wire containing 0 (a), 0.6 (b); 1.2 (c) and 2.5 wt% (d) of aluminum oxide.

As noted above, alumina is considered not to be a non-metallic inclusion, which is potentially active for the formation of acicular ferrite, however, as can be seen in Fig. 4d, in the structure with the maximum aluminum oxide content (2.5%) there is a significant volume fraction of intragranular acicular ferrite (IF) (Fig. 4, d). Taking into account the wide spectra of polymorphous modifications of alumina, the activity of nonmetallic inclusion for the nucleation of acicular ferrite may be caused not only by its chemical composition, but also by the crystal structure, and this question requires further consideration. In addition, as it is known, the probability of needle-like ferrite nucleation on nonmetallic inclusions increases sharply with the increase in the size of nonmetallic particles up to 1-2 μm. Apparently, at high temperatures the agglomeration and sintering of nanoscale alumina particles occurred to form larger particles that served as nucleation centers for acicular ferrite.

In Fig. 5, microhardness profiles along the welded seam up to the base metal are given. There is an obvious correlation of the values of hardness with the microstructure. The weld with the bainitic-martensitic structure (Fig. 3(a), 4(a)) obtained with the use of welded wire without the addition of oxide has the maximum hardness. The structure with a high volume fraction of polyhedral ferrite has the minimum hardness (Fig. 3(d), 4(d)) obtained with the maximum content of aluminum oxide.

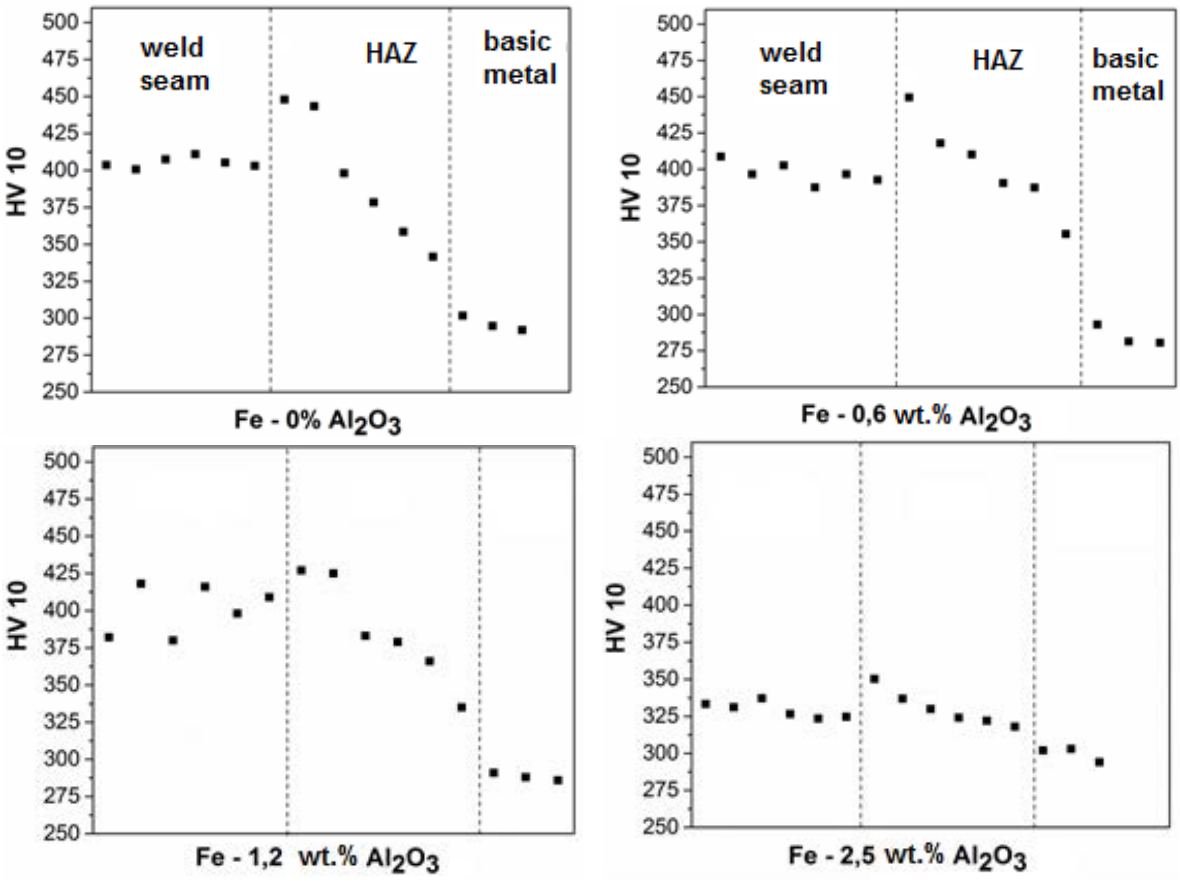

Fig. 5. Microhardness profile through the zones of weld.

Figure 6 shows the values of the microhardness of the welded seam, depending on the content of aluminum oxide in the welded wire. The hardness of the welded samples at alumina content from 0 to 1.2 mass% is almost 1.5 times higher than the hardness of the base material, which is due to the formation of a nonequilibrium bainitic martensitic structure due to the high cooling rate. When the aluminum oxide content is 2.5 mass%, the hardness of the welded material is higher than the hardness of the base material by only 10%.

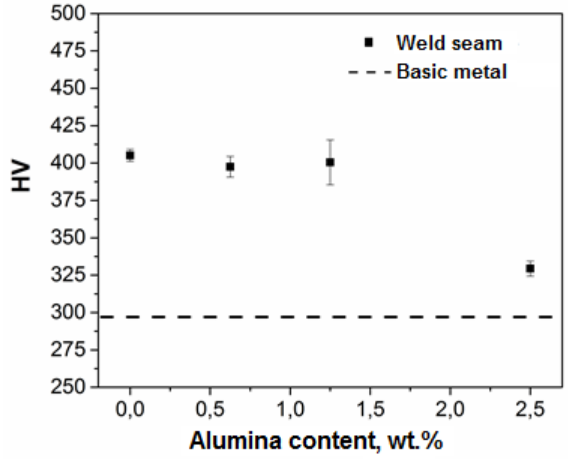

Fig. 6. Dependence of the microhardness of the welded joint on the content of aluminum oxide in the welding wire.

4. Conclusions

The main effect of alumina additions to the welding wire is the coarsening of the weld metal structure, which is apparently connected with a significant change in the thermophysical characteristics of the electrode and the weld pool. It is shown that the addition of alumina to the welding wire led to the initiation of the formation of intragranular acicular ferrite in the welded material, and the effect of dispersed hardening due to the inhibition of grain growth and movement of dislocations is not pronounced, which on the whole resulted in a more even distribution of hardness over the zones of the welded seam.

Acknowledgments*. The authors would like to thank the Russian Foundation for Basic Research (RFBR) (Grant no: 16-58-76008\17) for providing financial support in the frames of collaborative project "Nano Wire CWM" of ERA.Net RUS Plus program.*

References

[1] G. Sundararajan, R. Vijay and A.V. Reddy // *Cur. Sci*. **105** (2013) 8.
[2] D.W. Lee, O. Tolochko, C.J. Choi and B.K. Kim // *Powder Metall*. **45** (2002) 3.
[3] Y.S. Xu et al. // *Advanced Materials Research* **887-888** (2014) 32.
[4] K.A. Darling, M. Kapoor, H. Kotan, B.C. Hornbuckle, S.D. Walck, G.B. Thompson, M.A. Tschopp, L.J. Kecskes // *J. Nucl. Mater*. **467** (2015) 205.
[5] B. Beidokhti, A.H. Koukabi, A. Dolati // *Mater. Charact.* **60** (2009) 225.
[6] M.V. Abramov, S.B. Maslenkov, V.B. Kireev // *Metallovedenie i termicheskaya obrabotka metallov (Metal Science and Heat Treatment of Metals)* **2** (1981) 59.
[7] M. Fattahi, N. Nabhani, M.R. Vaezi, E. Rahimi // *Mater. Sci. Eng. A* **528** (2011) 8031.
[8] B.A. Wang, N. Wang, Y.J. Yang, H. Zhong, M.Z. Ma, X.Y. Zhang, R.P. Liu // *Mater. Sci. Eng. A* **692** (2017) 168.
[9] M. Fattahi, N. Nabhani, E. Rafiee, M. Nasibi, E. Ahmadi, Y. Fattahi // *Mater. Chem. Phys*. **146** (2014) 105.
[10] M. Fattahi, N. Nabhani, M. Hosseini, N. Arabian, E. Rahimi // *Micron.* **45** (2013) 107.
[11] H. Bhadeshia and R. Honeycombe, *Steels: Microstructure and Properties* (Elsevier Ltd, 2017).
[12] S.S. Babu // *Current Opinion in Solid State and Materials Science* **8** (2004) 267.
[13] T. Pan, Z.-G. Yang, C. Zhang, B.-Z. Bai, H.-S. Fang // *Mater. Sci. Eng. A* **438–440** (2006) 1128.
[14] D. Loder, S.K. Michelic, C. Bernhard // *J. of Mater. Sci. Resear.* **6(1)** (2017) 24.
[15] N. Travitzky, P. Kumar, K.H. Sandhage, R. Janssen, N. Claussen // *Mater. Sci. Eng. A* **344** (2003) 245.